Published in final edited form as:

Transl Stroke Res. 2017 June ; 8(3): 234–243. doi:10.1007/s12975-016-0511-5.

MRI Characterization in the Acute Phase of Experimental Subarachnoid Hemorrhage

Dewei Guo, MD[1,2], **D. Andrew Wilkinson, MD**[1], **B. Gregory Thompson, MD**[1], **Aditya S. Pandey, MD**[1], **Richard F Keep, PhD**[1], **Guohua Xi, MD**[1], and **Ya Hua, MD**[1,*]

[1] Department of Neurosurgery, University of Michigan, Ann Arbor, MI, USA

[2] Department of Neurosurgery, the Frist Affiliated Hospital of Zhengzhou University, Zhengzhou, China

Abstract

A number of mechanisms have been proposed for the early brain injury after subarachnoid hemorrhage (SAH). In this study, we investigated the radiographic characteristics and influence of gender on early brain injury after experimental SAH.

SAH was induced by endovascular perforation in male and female rats. Magnetic resonance imaging was performed in a 7.0-T Varian MR scanner at 24 hours after SAH. The occurrence and size of T2 lesions, ventricular dilation and white matter injury (WMI) was determined on T2 weighted images (T2WI). The effects of SAH on heme oxygenase-1 and fibrin/fibrinogen were examined by Western blotting and immunohistochemistry. SAH severity was assessed using a MRI grading system and neurological function was evaluated according to a modified Garcia's scoring system. T2-hyperintensity areas and enlarged ventricles were observed in T2WI coronal sections 24 hours after SAH. The overall incidence of T2-lesions, WMI and hydrocephalus was 54, 20 and 63%, respectively. Female rats had a higher incidence of T2-hyperintensity lesions and hydrocephalus, as well as larger T2 lesion volumes and higher average ventricular volume. SAH rats graded at 3-4 (our previously validated MRI grading scale) had larger T2 lesion volumes, more hydrocephalus and worse neurological function compared with those graded at 0-2.

In conclusion, T2-lesion, WMI and hydrocephalus were the most prevalent MRI characteristics 24 hours after experimental SAH. The T2-lesion area matched with fibrinogen/fibrin positive staining in the acute phase of SAH. SAH induced more severe brain injury in females compared to males in the acute phase of SAH.

Keywords

MRI; subarachnoid hemorrhage; white matter injury; hydrocephalus

* Corresponding Author: Ya Hua, MD, 5018 BSRB, University of Michigan, 109 Zina Pitcher Place, Ann Arbor, MI 48109-2200, USA, Telephone: (734) 764-1207, Fax: +1-734-763-7322, yahua@umich.edu.

Conflicts of Interest: Dewei Guo, Andrew Wilkinson, B. Gregory Thompson, Aditya S. Pandey, Richard F Keep, Guohua Xi, and Ya Hua declare that they have no conflict of interest.

Compliance with Ethics Requirements: All institutional and national guidelines for the care and use of laboratory animals were followed.

Introduction

Subarachnoid hemorrhage (SAH) is a devastating disease resulting in high mortality, especially within the first few days after aneurysm rupture(1, 2). However, the mechanism of brain injury during the acute period remains poorly understood and therapeutic options are limited(3, 4). MRI is a non-invasive method for collecting structural, physiological and functional imaging data with high spatial resolution (5). It has been widely used for detecting brain injuries such as cerebral edema, acute hydrocephalus (6-8), white matter injury (9-11) and ischemic lesions (12, 13) caused by various central nervous system diseases. However, due to longer acquisition time and difficulty in performing of MRI compared to CT scans and the high risk of re-bleeding in SAH patients, MRI is rarely performed clinically for the patients in the acute setting after SAH. In the current study, MRI was performed to examine SAH-induced acute hydrocephalus, white and grey matter injury in a rat model.

SAH occurs more frequently and with a higher incidence of hydrocephalus in women than in men (14-17). Our previous study indicated that the incidence of acute hydrocephalus after experimental SAH was also significantly greater in female rats (75%) than in males (47%) (6). This study examines the effect of gender on MRI findings and neurologic outcomes after SAH in rats.

Additionally, iron plays an important role in brain injury after experimental intracerebral hemorrhage (ICH) (18-20), intraventricular hemorrhage (IVH) (21, 22) and SAH (23). Our previous studies indicated that iron levels in CSF increase almost 14-fold after ICH on the third day, and remain high for at least one month after experimental ICH. Increases of brain iron levels cause brain edema, oxidative stress, brain atrophy and neurological deficits following ICH (18, 24, 25). After SAH, the brain is exposed to high concentrations of hemoglobin as erythrocytes lyse (26). Hemoglobin and heme are then captured by macrophages in the form of hemoglobin-haptoglobin and heme-hemopexin complexes via the hemoglobin scavenger receptor CD163 and hemopexin scavenger receptor CD91, respectively (27, 28). Heme-oxygenase-1 (HO-1) is a key inducible enzyme for heme degradation and iron release. The released iron can be stored in ferritin (18, 23, 29). An iron chelator, deferoxamine, effectively reduced iron and HO-1 levels and ameliorated acute neuronal injury after SAH (23). In this study, all experimental SAH rats were graded into 0-4 groups based on blood accumulation in the subarachnoid space. The relationship between MRI grading system after SAH and brain injury severity was determined.

Materials and Methods

Animal preparation and SAH induction

Animal use protocols were approved by the University of Michigan Committee on the Use and Care of Animals. Animals were housed under standard 12:12 light-dark conditions and allowed free access to water and food. A total of 148 (90 males and 58 females) adult Sprague-Dawley rats were used in this study of which 124 (n=76 in male group and n=48 in female group) had a SAH induced by endovascular perforation as previously described. (23). In brief, rats were anesthetized with 5% isoflurane. After intubation and initiation of

mechanical ventilation, isoflurane was maintained at 2.5-3%. After this, the left external carotid artery was identified under a surgical microscope, transected distally, and reflected caudally in line with the internal carotid artery. A 4-0 nylon monofilament suture was inserted into the stump of the external carotid artery through the common carotid artery bifurcation and into the internal carotid artery. The filament was advanced distally into the intracranial internal carotid artery to cause a vascular perforation. The filament was then withdrawn. The other 24 rats underwent a sham operation, the same procedure without perforation (n=14 in male group and n=10 in female group). Mortality rates were 24% (18 of 76) in male rats and 27% (13 of 48) in female rats at 24 hours after SAH. No death occurred after sham operations.

MRI and measurements

MRI imaging was performed in a 7.0-T Varian MR scanner (Varian Inc., Palo Alto, California) (30) 24 hours after induction of SAH. Rats had T2 fast spin-echo sequences (repetition time/echo time = 4,000/60 ms) and T2* gradient-echo sequences (repetition time/echo time = 250/5 ms) using a field of view of 35×35 mm, matrix of 256×256 mm and 25 coronal slices (0.5 mm thick). All MRI data analysis was performed by a blinded observer using NIH Image J software. T2-lesion volumes were measured as previously described (31). In brief, T2-lesion areas were identified using the mean value comparison between ipsi- and contralateral brain. A pixel in the ipsilateral of the brain was considered abnormal if its value was larger than the mean value plus twice the standard deviation provided by the contralateral brain. T2-lesion volumes were measured by combining abnormal pixels over all slices and multiplying by section thickness and were presenting as the volume ratio between T2-lesion and ipsilateral hemisphere. Ventricular and white matter injury volumes were measured and calculated as described previously (6, 7, 32). Ventricular volume is presented as the percentage of the mean in sham animals. Hydrocephalus was defined as ventricular volume over +3 standard deviations (SD) of the mean in sham animals (with separate values determined for males and females). To calculate the volume of white matter injury, the area of white matter T2-hyperintensity was measured in all slices and multiplied by section thickness.

SAH Grading in MRI

SAH severity score was assessed using MRI as previously described (33). In brief, 5 grades were categorized according to the thickness of SAH clot and the presence of IVH in the lateral ventricle: grade 0: no SAH or intraventricular hemorrhage (IVH); grade 1: minimal or thin SAH without IVH; grade 2:minimal or thin SAH with IVH; grade 3: thick SAH without IVH; grade 4: thick SAH with IVH. Thick SAH was defined as there being at least two slices with clots thicker than 0.5 mm on T2* MRI. IVH was defined as at least one hypointensity clot recognized in any ventricle on T2* imaging. Animals were divided into three groups: sham, mild SAH (grade 0-2) and severe SAH (grade 3-4) based on those criteria.

Neurological score

Neurological deficits were evaluated at 24 h after SAH by a blinded observer according to the modified Garcia's scoring system (34, 35). The neurobehavioral tests included: (1)

spontaneous activity, (2) symmetry in forelimb movement, (3) forepaw outstretching, (4) climbing, (5) body proprioception, and (6) response to vibrissae touch. Each test was assigned a score from 0 to 3. The minimum neurological score is 2 and the maximum is 18.

Immunohistochemistry

Rats were anesthetized with pentobarbital (60 mg/kg, i.p.) and underwent transcardiac perfusion with 4% paraformaldehyde in 0.1 mol/L (pH 7.4) phosphate-buffered saline. Brains were removed and kept in 4% paraformaldehyde for 6 h, then immersed in 30% sucrose for 3 to 4 days at 4 °C. Brains were then placed in optimal cutting temperature embedding compound (Sakura Finetek, Inc., Torrance, CA, U.S.A.) and sectioned on a cryostat (18 μm thick slices).

Immunohistochemistry was performed using avidin-biotin complex technique (36, 37). The primary antibodies were rabbit anti-HO-1 (1:400 dilution; Abcam) and rabbit anti-fibrinogen (1:200; Abcam). Coronal sections were stained with hematoxylin and eosin (H&E) for histopathologic evaluation. Lesion areas on the H&E stained sections (presented as percentage of ipsilateral hemisphere) were outlined and measured on a fixed section (bregma = −0.80mm) for each rat, which matched the MRI slice.

Western blot analysis

Western blot analysis was performed as previously described (23, 36, 38). Briefly, rats were perfused with 0.1mmol/L phosphate buffered saline (pH 7.4) after euthanasia and the ipsi- and contralateral cortex, white matter (corpus callosum) and basal ganglia were sampled. Protein concentration was determined by Bio-Rad protein assay kit (Hercules, CA) and 50 g protein of each sample was separated by SDS-PAGE and transferred onto a hybond-C pure nitrocellulose membrane (Amersham, Pittsburgh, PA). Polyclonal rabbit anti-HO-1 IgG (dilution 1:2000) antibody was used.

Statistical Analysis

The values are presented as means ± SD. Statistical differences in T2-lesion, hydrocephalus and WMI volume among different gender groups were analyzed using one-way ANOVA test. Statistical differences of the injury between mild and severe SAH groups were analyzed by Student's *t*-test. A chi-square test was used to determine the incidence differences as well as the correlations of T2-lesion, hydrocephalus and WMI among these groups. Spearman's rank correlation was used to examine correlations between T2-lesion volume and Garcia's score; MRI grading and ventricular volume, T2-lesion volume or WMI volume. Statistical significance was set as $p<0.05$.

Results

Brain injuries after SAH

T2-hyperintensity area in the brain parenchyma (T2-lesion), T2-hyperintensity in the corpus callosum (WMI) and enlarged ventricles (hydrocephalus when it is over +3 SD of the mean in sham animals) were found on T2WI after SAH (Fig. 1A). The overall incidence of T2-lesions after SAH was 54% (50/93) at 24 hours, hydrocephalus occurred in 63% (59/93)

while 20% (19/93) had white matter injury (Fig. 1B). The latter is different than a previous mouse study where all SAH animals had WMI (9). The lesion areas on T2WI consistently matched lesions identified on H&E staining. In addition, fibrinogen/fibrin-positive microthromboses were found in SAH rats with T2-lesions and the lumen of numerous arterioles were filled with erythrocytes and microthrombi (Fig. 2A). The basal ganglia of SAH rats had higher HO-1 immunoreactivity than sham-operated rats. The HO-1-positive cells and protein levels were much higher in the rats that had T2-lesions at 24 hours than those that had no T2-lesion ($p<0.05$; Fig. 2B).

SAH-induced more severe brain injuries in females than in males

Ventricular volumes were similar in female (11.2 ± 1.8 mm^3, n=10) and male (11.4 ± 2.7 mm^3, n=14) rats at 24 hours after the sham operation ($p=0.24$). But, SAH induced significantly ventricular enlargement (35.8 ± 15.8 mm^3 in females, n=35, $p<0.01$ and 25.3 ± 16.8mm^3 in males, n=58; $p<0.05$) compared to sham-operated rats. SAH-induced ventricular enlargement (expressed as a percentage of sham-operation values) was significantly larger in females (320 ± 141%, n=35) than in males (222 ± 147%, n=58, $p<0.01$, Fig. 3A, B). Acute hydrocephalus was defined as ventricular volume over +3SD of the mean in sham rats. Such acute hydrocephalus at 24 hours after SAH occurred more frequently in female than in male rats (89%, 31/35 vs. 48%, 28/58, respectively; $p<0.01$; Fig. 3C).

No T2-lesions or WMI were detected in sham-operated rats. The T2-lesion size (% of ipsilateral hemisphere) was markedly greater in female (14.2 ± 15.4%; n=35) than in male (7.1 ± 10.8%; n=58; $p<0.05$) rats (Fig. 3C). The incidence of T2-lesion at 24 hours after SAH was higher in female (69%, 24/35) than in male rats (45%, 26/58, $p<0.05$). There was a trend towards higher WMI volume in females compared to males, but this did not reach significance (3.4 ± 8.1mm^3; n=35 in female vs. 1.1 ± 4.0 mm^3; n=58 in male; $p=0.067$, Fig. 3D). The frequency of WMI at 24 hours after SAH was significantly higher in female (34%; 12/35) than in male (12%; 7/58) rats ($p=0.01$, Fig. 3D).

The correlation of brain injuries with MRI grading

Severity of brain injury, as assessed by ventricular enlargement, T2-lesion and WMI volumes , correlated with a MRI grading scale as indicated by our previous study (33) (Fig. 4A). The ventricular volume of SAH rats with higher grade SAH (283 ± 160%; n=68) was larger than that of rats with low SAH grade (193 ± 107%; n=25, $p<0.05$, Fig. 4B). The ratio of SAH-induced occurrence of hydrocephalus was also greater in high-grade SAH rats (72%, 49/68) than in low-grade SAH rats (40%, 10/25, $p<0.05$, Fig. 4E). There were significantly larger T2-lesion volumes (12.7 ± 13.9% vs. 1.9 ± 5.6%, $p<0.01$) and greater T2-lesion occurrence (66% vs. 20% $p<0.01$) in high-grade than in low-grade SAH rats (Fig. 4C, 4E). Although WMI volume was not statistically different (2.5 ± 6.7 vs. 0.5 ± 2.6; $p=0.16$, Fig. 4D), the frequency of WMI was markedly greater in high-grade SAH rats (26%, 18/68) than in low-grade rats (4%, 1/25, $p<0.05$, Fig. 4D, 4E).

There was a strong correlation between T2-lesion volume and Garcia's score ($r=0.64$, $p<0.05$; Fig. 5A). Correlations were also found between MRI grading and ventricular

volume (r=0.37, p<0.05; Fig. 5B), T2-lesion volume (r=0.45, p<0.05; Fig. 5C) and WMI volume (r=0.29, p<0.05; Fig. 5D). Of the SAH rats, 45% (42/93) had T2-lesion with hydrocephalus, and 18% (17/93) of them had a T2-lesion, hydrocephalus and white matter injury. The occurrence of T2-lesion, hydrocephalus and WMI correlated with each other (p<0.01 for T2-lesion and hydrocephalus; p<0.01 for T2-lesion and WMI; p<0.05 for hydrocephalus and WMI, Fig. 1A, 5E).

Discussion

MR imaging has well-documented advantages and reliability compared with CT in detecting cerebral edema, acute hydrocephalus (6-8), white matter injury (9-11) and ischemic lesions (12, 13). Imaging in the acute phase of SAH presentation may lead to better delineation of the early brain injury caused by SAH. However, MRI is usually not used in the acute phase of SAH as patients require critical care monitoring and MRI requires longer imaging time with minimal clinical monitoring (39, 40).

Early brain injury, which begins within minutes after aneurysms rupture (41), is believed to be a precursor for both delayed vasospasm and delayed ischemic neurological deficits (42). Our previous study showed that intracranial pressure (ICP) increased very rapidly after endovascular perforation, being markedly elevated within 0.5 minutes and, while there was some decrease by 20 min, it remained elevated for at least 60 min. Although there was a transient increase in blood pressure, the cerebral perfusion pressure (CPP) decreased very markedly immediately after SAH induction and, after a brief rebound, remained below the baseline for 60 minutes (26). The elevation of ICP and the reduction of CPP may lead to global cerebral ischemia. In this experimental study, 54% of SAH rats had a T2-lesions 24 hours after the endovascular perforation, with the lesion volume varying from 0.6 to 385 mm^3. All the observed T2-lesions were within the ipsilateral hemisphere adjacent to the puncture point where the anterior cerebral and middle cerebral arteries bifurcate. T2-lesions also occur clinically after SAH, but the lesion areas may be distributed in both hemispheres. This may be explained by the fact that the collateral circulation in rats is more robust than that in humans and thus the global rise in intracranial pressure post vessel/aneurysm rupture leads to more diffuse ischemic type changes within patients as compared to rats. The T2 changes adjacent to the rupture site are most likely associated with high flow blood causing traumatic cerebral injury (43). The global ischemia in SAH patients is further supported by a long-term follow-up MRI imaging study post SAH revealing that 81% of 104 patients presented a total of 152 areas of increased signal intensity on T2WI, which were consistent with previous infarction (12).

In the acute phase, the leading causes of T2-lesion are transient global ischemia induced by sharply elevated of intracranial pressure, microcirculatory constriction, microthrombosis, blood brain barrier disruption and high intracellular iron content (23, 42, 44, 45). In addition, H&E staining showed that the lesion areas on T2WI matched with histologic lesions (Fig. 2A). Fibrinogen/fibrinogen-stained microthromboses were found preferentially in the T2-lesion area compared to non-lesion areas. In the T2-lesion areas, numerous arterioles were filled with erythrocytes packed in the lumen in microthrombi and were not rinsed out during perfusion fixation. These findings support that the T2-lesional areas show areas of cerebral

infarction, which is consistent with others studies (12). These infarctions appear distinct from those caused by delayed cerebral ischemia (DCI) that do not appear until a number of days after ictus (46).

The immunoreactivity of HO-1 is increased significantly after experimental SAH. This may lead to an increase in brain nonheme iron, oxidative deoxyribonucleic acid injury, and ultimately neuronal death. An iron chelator, deferoxamine, has been shown to effectively reduce iron and HO-1 levels and ameliorate acute neuronal injury after SAH (23). In this study, HO-1 expression was significantly increased in T-2 lesion areas, suggesting that iron and iron handling proteins are associated with the formation of T2-lesion.

Acute hydrocephalus has been reported in 20% of patients within 72 hours after aneurysmal SAH. The occurrence of acute hydrocephalus was related to thickness of hematoma in the ventricle (47). We previously found a hydrocephalus incidence of 44% (12/27) in male rats (7). In the current study, the incidence was 63% (59/93) and correlated well with SAH severity.

Haptoglobin binding of hemoglobin represents a first line of defense line against hemolysis, facilitating removal of hemoglobin by CD163. However, this pathway may be saturated after SAH, leading to free hemoglobin in the cerebrospinal fluid. The increased red blood cell lysis, hemoglobin, heme and iron in cerebrospinal fluid may result in ventricular enlargement (48, 49).

White matter injury occurs in a variety neurologic diseases (50). Our previous study found that all wild type mice had abnormalities in white matter areas (corpus callosum, external capsule, or fimbriae) on T2WI 24 hours after SAH. These abnormalities correlated with axonal damage, myelin degradation and blood-brain barrier disruption (9). These findings are supported by a recent study (51). In contrast, in the current study, 20% of all rats showed an abnormality along the corpus callosum on T2WI 24 hours after SAH. There was a trend towards larger volume of white matter injury in female rats, though this did not reach significance (p=0.067 for male versus female).

The relationship between gender and cerebral hemorrhage has been examined previously both clinically (52, 53) and experimentally (54-56). We previously found that acute hydrocephalus occurs more frequently in female rats after SAH (6). In the current study, female rats had higher rates of SAH-induced T2-lesions and hydrocephalus. Female rats also had significantly larger T2 lesion volumes and greater ventricular enlargement compared to male rats. No significant differences in WMI volume on T2WI were observed between male and female rats after SAH, though there was a trend (p=0.067) towards larger volumes in female rats.

In clinical studies, women have been found to have a higher incidence of SAH and subsequent acute hydrocephalus (14-17), but the reason is still unknown. There is growing evidence that estrogen has an important influence on vascular physiology and the pathophysiology of cerebral aneurysms. It is involved in the formation and rupture of cerebral aneurysm and subsequent SAH (57, 58). The peak incidence of aneurysmal SAH occurs in the 7^{th} decade in women and the 6^{th} decade in men (59). Estrogen deficiency, such

as after menopause, is associated with increased risk for SAH (60) and hormone replacement therapy is associated with decreased risk SAH as well as ameliorating subsequent brain injury (52, 58, 61). However, no significant difference of overall outcomes after aneurysmal SAH was found between women and men in another study, despite differences in age and aneurysm characteristics (53). In animal models of other central nervous system injuries, such as traumatic brain injury (62, 63), intracerebral hemorrhage (54, 64), or ischemic stroke (65), estrogen plays a neuroprotective role, leading to less brain injury. The present study found that female rats had more evidence of brain injury than male rats 24 hours after SAH. In female rats, larger lesions and ventricular volumes as well as a higher incidence of lesions and hydrocephalus were observed on T2WI. The incidence of WMI was higher in female rats compared to males, and there was a non-significant trend towards higher WMI volumes in female rats compared to males.

One possible mechanism for the gender difference is that the activation of estrogen receptor-β in aneurysms before rupture may have a protective effect on the vessel wall and lead to attenuation of tissue damage. The estrogen receptor-β is predominantly distributed in human intracranial aneurysms and cerebral arteries. Estrogen has a protective effect that can prevent aneurysms from rupture through the activation of ER-β in ovariectomized mice (55). However, in an ischemic stroke model, estrogen receptor-α knockout mice had smaller cortical infarction volumes compared with to mice, suggesting that loss of estrogen receptor-α does not enhance tissue damage in females and that this neuroprotective role does not depend on activation of estrogen receptor-α (56). There are few studies about the immunoreactivity of estrogen receptors after SAH. We previously found that iron deposition may lead to increased periventricular brain injury after SAH and IVH (7, 21). Estrogen may influence iron metabolism by modulating the hepcidin-ferroportin axis, which fundamentally governs global iron absorption, distribution, utilization and egress. A repression of ferroportin at the transcriptional level by estrogen was observed in another study and could result in intracellular iron accumulation (66, 67).

Both T2-lesion volume and ventricular dilation were significantly greater in rats with severe SAH compared to those with mild SAH. The incidence of T2-lesions as well as hydrocephalus was also significantly higher in the severe SAH group. This indicates a correlation between early brain injury and clot thickness which reflects hemorrhage accumulation in the ventricles and cisterns. We previously found that the amount of subarachnoid blood or presence of intraventricular hemorrhage may cause obstruction of cerebrospinal fluid flow and lead to hydrocephalus (7). A clinical study found early ischemia in 40 of 61 (66%) of SAH patients using MRI. It was related to worse Hunt-Hess grade, GCS score and it significantly predicted an increased number and volume of infarcts on follow-up MRI (43). These findings indicate the potential utility of MRI in investigating early brain injury in experimental SAH studies without the need for animal euthanasia.

Conclusions

T2-lesions, white matter injury and hydrocephalus were the most prevalent MRI characteristics 24 hours after experimental SAH. Fibrinogen/fibrin was detected in T2-lesion

areas in the acute phase of SAH. Female rats developed more severe brain injury in the acute phase of SAH compared to males.

Acknowledgments

Disclosure: This study was supported by grants NS-073959, NS-079157, NS-090925, NS-084049, NS-091545, NS-096917 and NS-007222 from the National Institutes of Health (NIH). The content is solely the responsibility of the authors and does not necessarily represent the official views of the NIH.

References

1. Etminan N. Aneurysmal subarachnoid hemorrhage--status quo and perspective. Transl Stroke Res. Jun; 2015 6(3):167–70. PubMed PMID: 25860440. [PubMed: 25860440]
2. Macdonald RL, Pluta RM, Zhang JH. Cerebral vasospasm after subarachnoid hemorrhage: the emerging revolution. Nature clinical practice Neurology. May; 2007 3(5):256–63. PubMed PMID: 17479073d. Epub 2007/05/05. eng.
3. Zhang JH. Vascular neural network in subarachnoid hemorrhage. Transl Stroke Res. Aug; 2014 5(4): 423–8. PubMed PMID: 24986148. Pubmed Central PMCID: 4127639. [PubMed: 24986148]
4. Tso MK, Macdonald RL. Subarachnoid hemorrhage: a review of experimental studies on the microcirculation and the neurovascular unit. Transl Stroke Res. Apr; 2014 5(2):174–89. PubMed PMID: 24510780. [PubMed: 24510780]
5. Sun Y, Shen Q, Watts LT, Muir ER, Huang S, Yang GY, et al. Multimodal MRI characterization of experimental subarachnoid hemorrhage. Neuroscience. Mar 1.2016 316:53–62. PubMed PMID: 26708744. Pubmed Central PMCID: PMC4724533. [PubMed: 26708744]
6. Shishido H, Zhang H, Okubo S, Hua Y, Keep RF, Xi G. The Effect of Gender on Acute Hydrocephalus after Experimental Subarachnoid Hemorrhage. Acta Neurochir Suppl. 2016; 121:335–9. PubMed PMID: 26463971. [PubMed: 26463971]
7. Okubo S, Strahle J, Keep RF, Hua Y, Xi G. Subarachnoid hemorrhage-induced hydrocephalus in rats. Stroke. Feb; 2013 44(2):547–50. PubMed PMID: 23212164. Pubmed Central PMCID: 3552015. Epub 2012/12/06. eng. [PubMed: 23212164]
8. Tiebosch IA, van den Bergh WM, Bouts MJ, Zwartbol R, van der Toorn A, Dijkhuizen RM. Progression of brain lesions in relation to hyperperfusion from subacute to chronic stages after experimental subarachnoid hemorrhage: a multiparametric MRI study. Cerebrovasc Dis. 2013; 36(3):167–72. PubMed PMID: 24135525. [PubMed: 24135525]
9. Egashira Y, Hua Y, Keep RF, Xi G. Acute white matter injury after experimental subarachnoid hemorrhage: potential role of lipocalin 2. Stroke. Jul; 2014 45(7):2141–3. PubMed PMID: 24893611. Pubmed Central PMCID: 4074774. [PubMed: 24893611]
10. Kummer TT, Magnoni S, MacDonald CL, Dikranian K, Milner E, Sorrell J, et al. Experimental subarachnoid haemorrhage results in multifocal axonal injury. Brain. Sep.2015 138:2608–18. Pt 9. PubMed PMID: 26115676. Pubmed Central PMCID: PMC4564022. [PubMed: 26115676]
11. Egashira Y, Hua Y, Keep RF, Iwama T, Xi G. Lipocalin 2 and Blood-Brain Barrier Disruption in White Matter after Experimental Subarachnoid Hemorrhage. Acta Neurochir Suppl. 2016; 121:131–4. PubMed PMID: 26463936. [PubMed: 26463936]
12. Kivisaari RP, Salonen O, Servo A, Autti T, Hernesniemi J, Ohman J. MR imaging after aneurysmal subarachnoid hemorrhage and surgery: a long-term follow-up study. AJNR Am J Neuroradiol. Jun-Jul;2001 22(6):1143–8. PubMed PMID: 11415911. [PubMed: 11415911]
13. Shimoda M, Takeuchi M, Tominaga J, Oda S, Kumasaka A, Tsugane R. Asymptomatic versus symptomatic infarcts from vasospasm in patients with subarachnoid hemorrhage: serial magnetic resonance imaging. Neurosurgery. Dec; 2001 49(6):1341–8. discussion 8-50. PubMed PMID: 11846933. [PubMed: 11846933]
14. Longstreth WT Jr. Koepsell TD, Yerby MS, van Belle G. Risk factors for subarachnoid hemorrhage. Stroke. May-Jun;1985 16(3):377–85. PubMed PMID: 3890278. [PubMed: 3890278]
15. Rothwell PM, Coull AJ, Silver LE, Fairhead JF, Giles MF, Lovelock CE, et al. Population-based study of event-rate, incidence, case fatality, and mortality for all acute vascular events in all arterial

territories (Oxford Vascular Study). Lancet. Nov 19; 2005 366(9499):1773–83. PubMed PMID: 16298214. [PubMed: 16298214]

16. Kongable GL, Lanzino G, Germanson TP, Truskowski LL, Alves WM, Torner JC, et al. Gender-related differences in aneurysmal subarachnoid hemorrhage. J Neurosurg. Jan; 1996 84(1):43–8. PubMed PMID: 8613834. [PubMed: 8613834]
17. van Asch CJ, van der Schaaf IC, Rinkel GJ. Acute hydrocephalus and cerebral perfusion after aneurysmal subarachnoid hemorrhage. AJNR Am J Neuroradiol. Jan; 2010 31(1):67–70. PubMed PMID: 19850767. [PubMed: 19850767]
18. Xi G, Keep RF, Hoff JT. Mechanisms of brain injury after intracerebral haemorrhage. Lancet Neurol. Jan; 2006 5(1):53–63. PubMed PMID: 16361023. [PubMed: 16361023]
19. Xiong XY, Yang QW. Rethinking the roles of inflammation in the intracerebral hemorrhage. Transl Stroke Res. Oct; 2015 6(5):339–41. PubMed PMID: 25940771. [PubMed: 25940771]
20. Zhao H, Garton T, Keep RF, Hua Y, Xi G. Microglia/Macrophage Polarization After Experimental Intracerebral Hemorrhage. Transl Stroke Res. Dec; 2015 6(6):407–9. PubMed PMID: 26446073. Pubmed Central PMCID: 4628553. [PubMed: 26446073]
21. Chen Z, Gao C, Hua Y, Keep RF, Muraszko K, Xi G. Role of iron in brain injury after intraventricular hemorrhage. Stroke. Feb; 2011 42(2):465–70. PubMed PMID: 21164132. Epub 2010/12/18. eng. [PubMed: 21164132]
22. Garton T, Keep RF, Wilkinson DA, Strahle JM, Hua Y, Garton HJ, et al. Intraventricular Hemorrhage: the Role of Blood Components in Secondary Injury and Hydrocephalus. Transl Stroke Res. Jun 30.2016 PubMed PMID: 27358176.
23. Lee JY, Keep RF, He Y, Sagher O, Hua Y, Xi G. Hemoglobin and iron handling in brain after subarachnoid hemorrhage and the effect of deferoxamine on early brain injury. J Cereb Blood Flow Metab. Nov; 2010 30(11):1793–803. PubMed PMID: 20736956. Pubmed Central PMCID: PMC2970675. [PubMed: 20736956]
24. Hua Y, Nakamura T, Keep RF, Wu J, Schallert T, Hoff JT, et al. Long-term effects of experimental intracerebral hemorrhage: the role of iron. J Neurosurg. Feb; 2006 104(2):305–12. PubMed PMID: 16509506.
25. Xi G, Strahle J, Hua Y, Keep RF. Progress in translational research on intracerebral hemorrhage: Is there an end in sight? Prog Neurobiol. Apr.2014 115C:45–63. PubMed PMID: 24139872. Pubmed Central PMCID: 3961535.
26. Lee JY, Sagher O, Keep R, Hua Y, Xi G. Comparison of experimental rat models of early brain injury after subarachnoid hemorrhage. Neurosurgery. Aug; 2009 65(2):331–43. discussion 43. PubMed PMID: 19625913. Epub 2009/07/25. eng. [PubMed: 19625913]
27. Soares MP, Hamza I. Macrophages and Iron Metabolism. Immunity. Mar 15; 2016 44(3):492–504. PubMed PMID: 26982356. Pubmed Central PMCID: PMC4794998. [PubMed: 26982356]
28. Garland P, Durnford AJ, Okemefuna AI, Dunbar J, Nicoll JA, Galea J, et al. Heme-Hemopexin Scavenging Is Active in the Brain and Associates With Outcome After Subarachnoid Hemorrhage. Stroke. Mar; 2016 47(3):872–6. PubMed PMID: 26768209. [PubMed: 26768209]
29. Gozzelino R, Soares MP. Coupling heme and iron metabolism via ferritin H chain. Antioxid Redox Signal. Apr 10; 2014 20(11):1754–69. PubMed PMID: 24124891. Pubmed Central PMCID: PMC3961798. [PubMed: 24124891]
30. Zhao J, Chen Z, Xi G, Keep RF, Hua Y. Deferoxamine Attenuates Acute Hydrocephalus After Traumatic Brain Injury in Rats. Transl Stroke Res. Jun 17.2014 5:586–94. PubMed PMID: 24935175. [PubMed: 24935175]
31. Li L, Jiang Q, Ding G, Zhang L, Zhang ZG, Ewing JR, et al. Map-ISODATA demarcates regional response to combination rt-PA and 7E3 F(ab')2 treatment of embolic stroke in the rat. J Magn Reson Imaging. Jun; 2005 21(6):726–34. PubMed PMID: 15906325. [PubMed: 15906325]
32. Ni W, Gao F, Zheng M, Koch LG, Britton SL, Keep RF, et al. Effects of Aerobic Capacity on Thrombin-Induced Hydrocephalus and White Matter Injury. Acta Neurochir Suppl. 2016; 121:379–84. PubMed PMID: 26463978. [PubMed: 26463978]
33. Shishido H, Egashira Y, Okubo S, Zhang H, Hua Y, Keep RF, et al. A magnetic resonance imaging grading system for subarachnoid hemorrhage severity in a rat model. J Neurosci Methods. Mar

30.2015 243:115–9. PubMed PMID: 25677406. Pubmed Central PMCID: PMC4359648. [PubMed: 25677406]

34. Garcia JH, Wagner S, Liu KF, Hu XJ. Neurological deficit and extent of neuronal necrosis attributable to middle cerebral artery occlusion in rats. Statistical validation. Stroke. Apr; 1995 26(4):627–34. discussion 35. PubMed PMID: 7709410. [PubMed: 7709410]
35. Jeon H, Ai J, Sabri M, Tariq A, Shang X, Chen G, et al. Neurological and neurobehavioral assessment of experimental subarachnoid hemorrhage. BMC Neurosci. 2009; 10:103. PubMed PMID: 19706182. Pubmed Central PMCID: PMC2749856. [PubMed: 19706182]
36. Zheng M, Du H, Ni W, Koch LG, Britton SL, Keep RF, et al. Iron-induced necrotic brain cell death in rats with different aerobic capacity. Transl Stroke Res. Jun; 2015 6(3):215–23. PubMed PMID: 25649272. Pubmed Central PMCID: 4425582. [PubMed: 25649272]
37. Song J, Li P, Chaudhary N, Gemmete JJ, Thompson BG, Xi G, et al. Correlating Cerebral (18)FDG PET-CT Patterns with Histological Analysis During Early Brain Injury in a Rat Subarachnoid Hemorrhage Model. Transl Stroke Res. Aug; 2015 6(4):290–5. PubMed PMID: 25833084. [PubMed: 25833084]
38. Wan S, Cheng Y, Jin H, Guo D, Hua Y, Keep RF, et al. Microglia Activation and Polarization After Intracerebral Hemorrhage in Mice: the Role of Protease-Activated Receptor-1. Transl Stroke Res. May 21.2016 PubMed PMID: 27206851.
39. Park J, Woo H, Kang DH, Kim YS, Kim MY, Shin IH, et al. Formal protocol for emergency treatment of ruptured intracranial aneurysms to reduce in-hospital rebleeding and improve clinical outcomes. J Neurosurg. Feb; 2015 122(2):383–91. PubMed PMID: 25403841. [PubMed: 25403841]
40. van Donkelaar CE, Bakker NA, Veeger NJ, Uyttenboogaart M, Metzemaekers JD, Luijckx GJ, et al. Predictive Factors for Rebleeding After Aneurysmal Subarachnoid Hemorrhage: Rebleeding Aneurysmal Subarachnoid Hemorrhage Study. Stroke. Aug; 2015 46(8):2100–6. PubMed PMID: 26069261. [PubMed: 26069261]
41. Nau R, Haase S, Bunkowski S, Bruck W. Neuronal apoptosis in the dentate gyrus in humans with subarachnoid hemorrhage and cerebral hypoxia. Brain Pathol. Jul; 2002 12(3):329–36. PubMed PMID: 12146801. [PubMed: 12146801]
42. Chen S, Feng H, Sherchan P, Klebe D, Zhao G, Sun X, et al. Controversies and evolving new mechanisms in subarachnoid hemorrhage. Prog Neurobiol. Apr.2014 115:64–91. PubMed PMID: 24076160. Pubmed Central PMCID: 3961493. [PubMed: 24076160]
43. Frontera JA, Ahmed W, Zach V, Jovine M, Tanenbaum L, Sehba F, et al. Acute ischaemia after subarachnoid haemorrhage, relationship with early brain injury and impact on outcome: a prospective quantitative MRI study. J Neurol Neurosurg Psychiatry. Jan; 2015 86(1):71–8. PubMed PMID: 24715224. [PubMed: 24715224]
44. Cahill J, Calvert JW, Zhang JH. Mechanisms of early brain injury after subarachnoid hemorrhage. J Cereb Blood Flow Metab. Nov; 2006 26(11):1341–53. PubMed PMID: 16482081. [PubMed: 16482081]
45. Sabri M, Lass E, Macdonald RL. Early brain injury: a common mechanism in subarachnoid hemorrhage and global cerebral ischemia. Stroke Res Treat. 2013; 2013:394036. PubMed PMID: 23533958. Pubmed Central PMCID: PMC3603523. [PubMed: 23533958]
46. Seder DB, Mayer SA. Critical care management of subarachnoid hemorrhage and ischemic stroke. Clin Chest Med. Mar; 2009 30(1):103–22. viii-ix. PubMed PMID: 19186283. [PubMed: 19186283]
47. van Gijn J, Hijdra A, Wijdicks EF, Vermeulen M, van Crevel H. Acute hydrocephalus after aneurysmal subarachnoid hemorrhage. J Neurosurg. Sep; 1985 63(3):355–62. PubMed PMID: 4020461. [PubMed: 4020461]
48. Gao C, Du H, Hua Y, Keep RF, Strahle J, Xi G. Role of red blood cell lysis and iron in hydrocephalus after intraventricular hemorrhage. J Cereb Blood Flow Metab. Jun; 2014 34(6): 1070–5. PubMed PMID: 24667910. Pubmed Central PMCID: 4050252. [PubMed: 24667910]
49. Strahle JM, Garton T, Bazzi AA, Kilaru H, Garton HJ, Maher CO, et al. Role of hemoglobin and iron in hydrocephalus after neonatal intraventricular hemorrhage. Neurosurgery. Dec; 2014 75(6):

696–705. discussion 6. PubMed PMID: 25121790. Pubmed Central PMCID: 4237659. [PubMed: 25121790]

50. Dewar D, Underhill SM, Goldberg MP. Oligodendrocytes and ischemic brain injury. J Cereb Blood Flow Metab. Mar; 2003 23(3):263–74. PubMed PMID: 12621301. [PubMed: 12621301]
51. Muroi C, Kashiwagi Y, Rokugawa T, Tonomura M, Obata A, Nevzati E, et al. Evaluation of a filament perforation model for mouse subarachnoid hemorrhage using 7.0 Tesla MRI. J Clin Neurosci. Jun.2016 28:141–7. PubMed PMID: 27021225. [PubMed: 27021225]
52. Qureshi AI, Malik AA, Saeed O, Defillo A, Sherr GT, Suri MF. Hormone replacement therapy and the risk of subarachnoid hemorrhage in postmenopausal women. J Neurosurg. Jan; 2016 124(1): 45–50. PubMed PMID: 26162033. [PubMed: 26162033]
53. Hamdan A, Barnes J, Mitchell P. Subarachnoid hemorrhage and the female sex: analysis of risk factors, aneurysm characteristics, and outcomes. J Neurosurg. Dec; 2014 121(6):1367–73. PubMed PMID: 25216063. [PubMed: 25216063]
54. Xie Q, Xi G, Keep RF, Hua Y. Effects of Gender and Estrogen Receptors on Iron-Induced Brain Edema Formation. Acta Neurochir Suppl. 2016; 121:341–5. PubMed PMID: 26463972. [PubMed: 26463972]
55. Tada Y, Wada K, Shimada K, Makino H, Liang EI, Murakami S, et al. Estrogen protects against intracranial aneurysm rupture in ovariectomized mice. Hypertension. Jun; 2014 63(6):1339–44. PubMed PMID: 24732889. Pubmed Central PMCID: PMC4034536. [PubMed: 24732889]
56. Sampei K, Goto S, Alkayed NJ, Crain BJ, Korach KS, Traystman RJ, et al. Stroke in estrogen receptor-alpha-deficient mice. Stroke. Mar; 2000 31(3):738–43. discussion 44. PubMed PMID: 10700513. [PubMed: 10700513]
57. Mhurchu CN, Anderson C, Jamrozik K, Hankey G, Dunbabin D, Australasian Cooperative Research on Subarachnoid Hemorrhage Study G. Hormonal factors and risk of aneurysmal subarachnoid hemorrhage: an international population-based, case-control study. Stroke. Mar; 2001 32(3):606–12. PubMed PMID: 11239175. [PubMed: 11239175]
58. Tabuchi S. Relationship between Postmenopausal Estrogen Deficiency and Aneurysmal Subarachnoid Hemorrhage. Behav Neurol. 2015; 2015:720141. PubMed PMID: 26538819. Pubmed Central PMCID: PMC4619901. [PubMed: 26538819]
59. Horiuchi T, Tanaka Y, Hongo K. Sex-related differences in patients treated surgically for aneurysmal subarachnoid hemorrhage. Neurol Med Chir (Tokyo). Jul; 2006 46(7):328–32. discussion 32. PubMed PMID: 16861825. [PubMed: 16861825]
60. Baron JA, La Vecchia C, Levi F. The antiestrogenic effect of cigarette smoking in women. Am J Obstet Gynecol. Feb; 1990 162(2):502–14. PubMed PMID: 2178432. [PubMed: 2178432]
61. Longstreth WT, Nelson LM, Koepsell TD, van Belle G. Subarachnoid hemorrhage and hormonal factors in women. A population-based case-control study. Ann Intern Med. Aug 1; 1994 121(3): 168–73. PubMed PMID: 8017743. [PubMed: 8017743]
62. Asl SZ, Khaksari M, Khachki AS, Shahrokhi N, Nourizade S. Contribution of estrogen receptors alpha and beta in the brain response to traumatic brain injury. J Neurosurg. Aug; 2013 119(2):353–61. PubMed PMID: 23724987. [PubMed: 23724987]
63. Khaksari M, Hajializadeh Z, Shahrokhi N, Esmaeili-Mahani S. Changes in the gene expression of estrogen receptors involved in the protective effect of estrogen in rat's trumatic brain injury. Brain Res. Aug 27.2015 1618:1–8. PubMed PMID: 26003937. [PubMed: 26003937]
64. Nakamura T, Hua Y, Keep RF, Park JW, Xi G, Hoff JT. Estrogen therapy for experimental intracerebral hemorrhage in rats. J Neurosurg. Jul; 2005 103(1):97–103. PubMed PMID: 16121980. [PubMed: 16121980]
65. Liu R, Yang SH. Window of opportunity: estrogen as a treatment for ischemic stroke. Brain Res. Jun 13.2013 1514:83–90. PubMed PMID: 23340160. Pubmed Central PMCID: PMC3664650. [PubMed: 23340160]
66. Qian Y, Yin C, Chen Y, Zhang S, Jiang L, Wang F, et al. Estrogen contributes to regulating iron metabolism through governing ferroportin signaling via an estrogen response element. Cell Signal. May; 2015 27(5):934–42. PubMed PMID: 25660146. [PubMed: 25660146]

67. Kim DK, Jeong JH, Lee JM, Kim KS, Park SH, Kim YD, et al. Inverse agonist of estrogen-related receptor gamma controls Salmonella typhimurium infection by modulating host iron homeostasis. Nat Med. Apr; 2014 20(4):419–24. PubMed PMID: 24658075. [PubMed: 24658075]

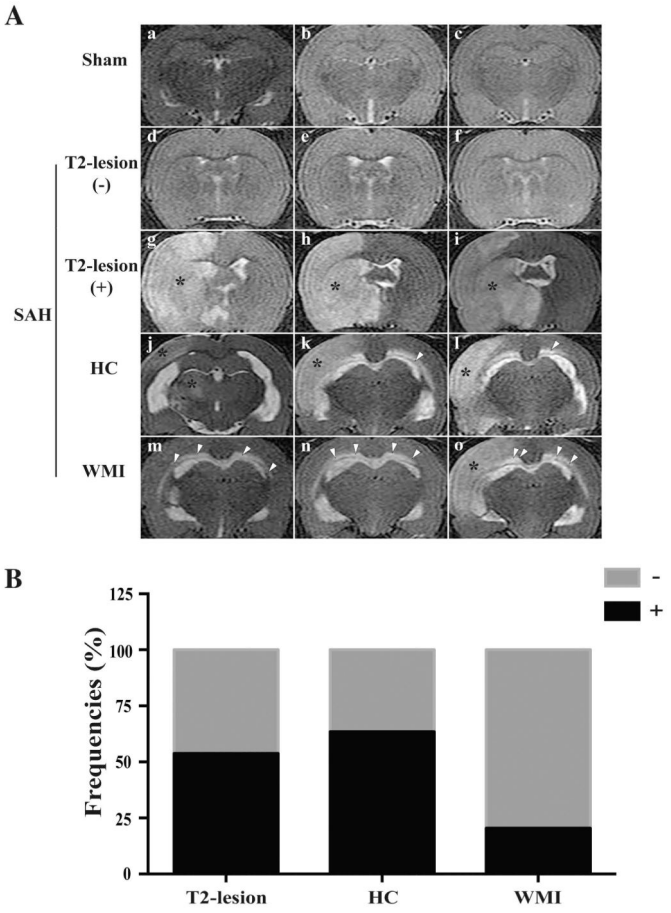

Fig. 1.

(A) T2-lesion (g-i, asterisk), hydrocephalus (HC; j-l) and WMI (m-o, arrowheads) in T2-weighted magnetic resonance imagines (MRI) in rats with a sham (a-c) or a SAH endovascular perforation operation (d-o) at 24 hours after procedure; **(B)** The overall incidence of T2-lesions, HC and WMI respectively 24 hours after endovascular perforation **(n=93)**.

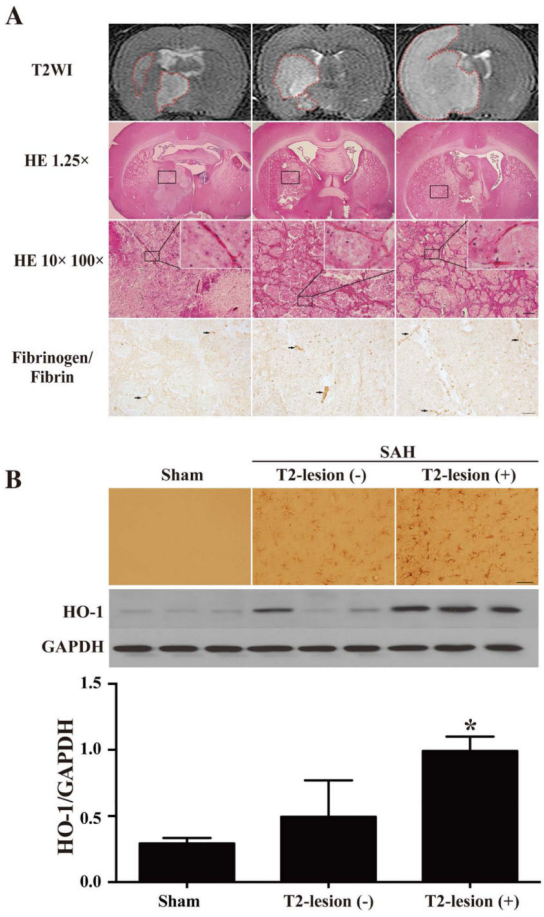

Fig. 2.

(A) The SAH-induced lesions in T2WI, by HE staining (scale bars = 1mm, 100 μm and 10 μm**; n=24**) and fibrinogen/fibrin immunostaining (scale bar = 20 μm); **(B)** The immunoreactivity and protein levels of HO-1 in sham or SAH operated rats, scale bar = 50 μm, **n=3,** * p<0.05.

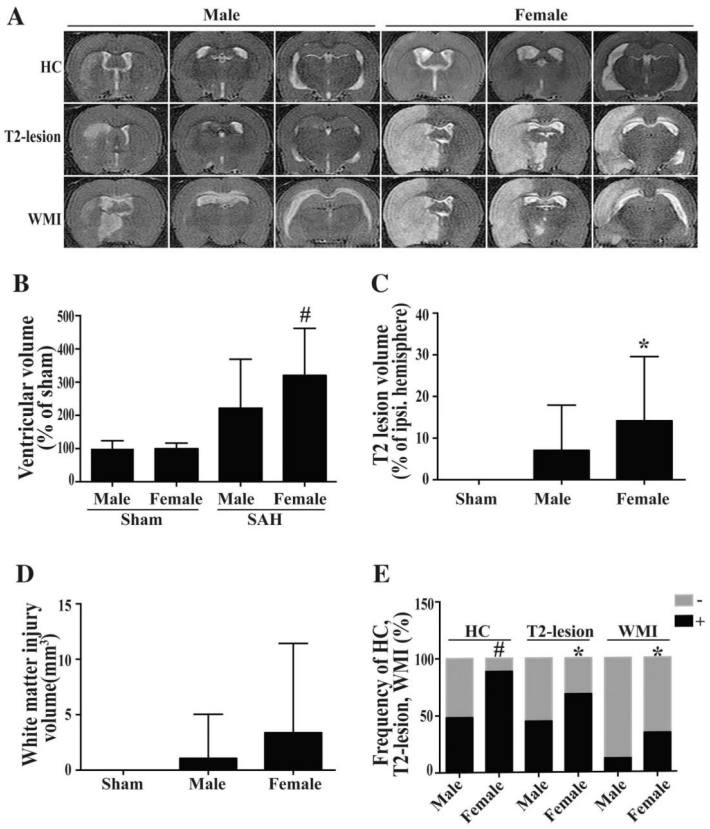

Fig. 3.

T2 weighted MRIs **(A)**; the volumes of ventricle **(B)**, T2 lesion **(C)** and white matter injury **(D)**; and the frequency of hydrocephalus (HC), T2-lesion and WMI **(E)** in male and female rats at 24 hours after SAH (male, n=58; female, n=35) or sham operation (male, n=14; female, n=10), # $p<0.01$, * $p<0.05$.

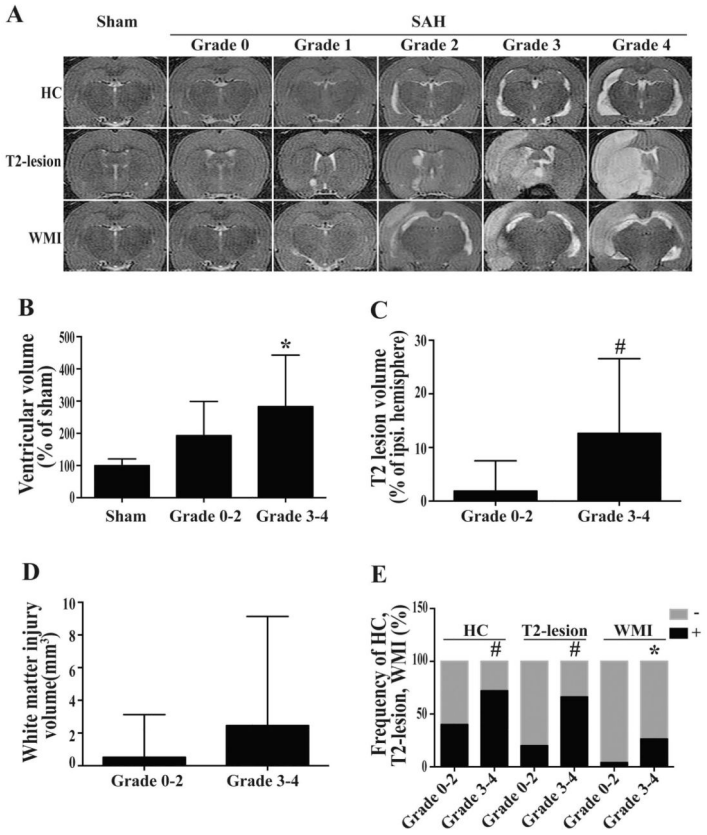

Fig. 4.

T2 weighted MRIs **(A)**; the volumes of ventricle **(B)**, T2 lesion **(C)** and white matter injury **(D)**; and the frequency of hydrocephalus (HC), T2-lesion and WMI **(E)** in rats with different SAH grades (Grade 0-2, n=27; Grade 3-4, n=66) or sham operation (n=24) at 24 hours after surgery, # $p<0.01$, * $p<0.05$.

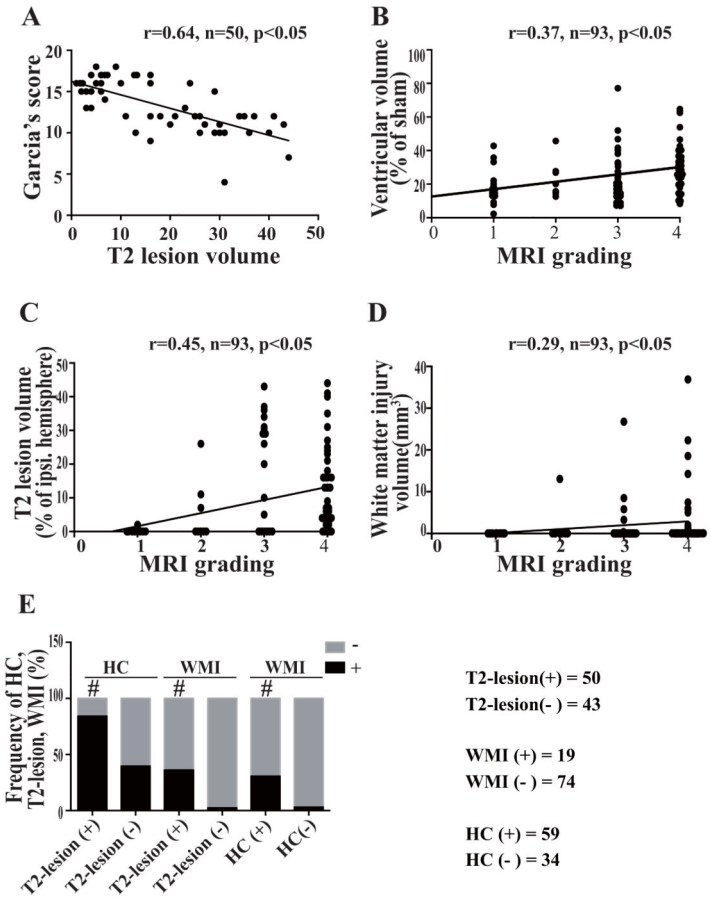

Fig. 5.

Correlations of neurological score and T2-lesion volume **(A)**; MRI grading with the volumes of ventricle **(B)**, T2-lesion **(C)** and WMI **(D);** and correlations of the occurrence of T2-lesion, hydrocephalus (HC) and WMI, # $p<0.01$.